



Sensitive electrochemical sensor using a graphene–polyaniline nanocomposite for simultaneous detection of Zn(II), Cd(II), and Pb(II)



Nipapan Ruecha^a, Nadnudda Rodthongkum^b, David M. Cate^c, John Volckens^{c,d}, Orawon Chailapakul^{e,f,**}, Charles S. Henry^{c,g,*}

^a Program in Macromolecular Science, Faculty of Science, Chulalongkorn University, Phayathai Road, Patumwan, Bangkok 10330, Thailand

^b Metallurgy and Materials Science Research Institute, Chulalongkorn University, Soi Chula 12, Phayathai Road, Patumwan, Bangkok 10330, Thailand

^c Department of Biomedical Engineering, Colorado State University, Fort Collins, Colorado 80523, USA

^d Department of Mechanical Engineering, Colorado State University, Fort Collins, Colorado 80523, USA

^e Electrochemistry and Optical Spectroscopy Research Unit (EOSRU), Department of Chemistry, Faculty of Science, Chulalongkorn University, Phayathai Road, Patumwan, Bangkok 10330, Thailand

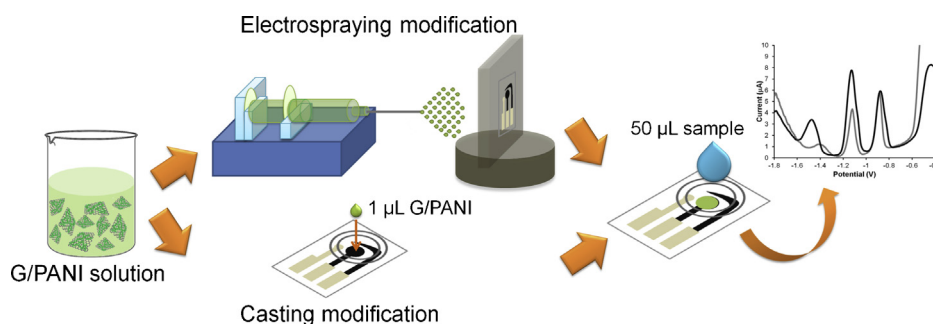
^f National Center of Excellence for Petroleum, Petrochemicals, Advanced Materials, Chulalongkorn University, Phayathai Road, Patumwan, Bangkok 10330, Thailand

^g Department of Chemistry, Colorado State University, Fort Collins, Colorado 80523, USA

HIGHLIGHTS

- Detection limits for Zn, Pb, and Cd using ASV were 1, 0.1, and 0.1 $\mu\text{g L}^{-1}$, respectively.
- G/PANI-modification led to a 3 \times improvement in signal vs. unmodified electrodes.
- ASV on a plastic substrate exhibited better sensitivity than on a paper substrate.
- Zn, Pb, and Cd were measured in human serum using method of standard addition.

GRAPHICAL ABSTRACT



ARTICLE INFO

Article history:

Received 28 December 2014

Received in revised form 18 February 2015

Accepted 24 February 2015

Available online 27 February 2015

Keywords:

Heavy metal
Paper-based devices
Point-of-need
Diagnostic
Pollution
Exposure

ABSTRACT

This work describes the development of an electrochemical sensor for simultaneous detection of Zn(II), Cd(II), and Pb(II) using a graphene–polyaniline (G/PANI) nanocomposite electrode prepared by reverse-phase polymerization in the presence of polyvinylpyrrolidone (PVP). Two substrate materials (plastic film and filter paper) and two nanocomposite deposition methods (drop-casting and electro spraying) were investigated. Square-wave anodic stripping voltammetry currents were higher for plastic vs. paper substrates. Performance of the G/PANI nanocomposites was characterized by scanning electron microscopy (SEM) and cyclic voltammetry. The G/PANI-modified electrode exhibited high electrochemical conductivity, producing a three-fold increase in anodic peak current (vs. the unmodified electrode). The G/PANI-modified electrode also showed evidence of increased surface area under SEM. Square-wave anodic stripping voltammetry was used to measure Zn(II), Cd(II), and Pb(II) in the presence of Bi(III). A linear working range of 1–300 $\mu\text{g L}^{-1}$ was established between anodic current and metal ion concentration with detection limits ($S/N = 3$) of 1.0 $\mu\text{g L}^{-1}$ for Zn(II), and 0.1 $\mu\text{g L}^{-1}$ for both

* Correspondence author at: Colorado State University Department of Chemistry, 1872 Campus Delivery, Fort Collins, CO 80523, USA. Tel.: +1 970 491 2852.

** Correspondence author at: Electrochemistry and Optical Spectroscopy Research Unit (EOSRU), Department of Chemistry, Faculty of Science, Chulalongkorn University, Phayathai Road, Patumwan, Bangkok 10330, Thailand.

E-mail addresses: orawon@chula.ac.th (O. Chailapakul), chuck.henry@colostate.edu (C.S. Henry).

Cd(II) and Pb(II). The G/PANI-modified electrode allowed selective determination of the target metals in the presence of common metal interferences including Mn(II), Cu(II), Fe(III), Fe(II), Co(III), and Ni(II). Repeat assays on the same device demonstrated good reproducibility (%RSD < 11) over 10 serial runs. Finally, this system was utilized for determining Zn(II), Cd(II), and Pb(II) in human serum using the standard addition method.

© 2015 Elsevier B.V. All rights reserved.

1. Introduction

Heavy metals have long been recognized as a significant threat to human and environmental health [1,2]. Human exposure (and intake) of heavy metals occurs through contaminated air, water, and food; these exposure pathways are complex and multifaceted. Quantifying metal concentrations in biological fluids such as blood, serum, or urine is of interest because abnormal levels can lead to both acute and chronic health problems [3].

Conventional measurement methods for metals include atomic absorption spectrophotometry [4], inductively-coupled-plasma mass spectrometry [5], and/or mass spectrometry [6]. Although these methods generally provide high selectivity and sensitivity, they are expensive and very difficult, if not impossible, to be completed in the field. Complicated operation and sample processing time also limit the number and throughout of measurements. Electrochemistry is an alternative detection method that has been incorporated in low-cost sensors for trace metal analysis [7–9]. Square-wave anodic stripping voltammetry is commonly used for metal detection due to its high sensitivity and low (\sim nM–pM) detection limits [10,11], a result of a pre-concentration step that accumulates metal on the electrode surface. The size and cost of benchtop potentiostats can be reduced using handheld devices, which can improve the utility of electrochemical detection in a point-of-need settings [10]. Glass, ceramic, and polymer substrates have been traditionally employed for electrochemical cells, however plastic commercial films (i.e., transparency film) are gaining traction due to their disposability, low cost, and chemical compatibility [12]. Another material, cellulose filter paper, is also being used for electrochemical sensing applications with greater frequency due to its high surface area and low cost [13,14] versus other traditional substrates (e.g., glass and ceramic) [15] as well its propensity for retaining chemical reagents for microfluidic assays [12].

A variety of electrode surface modifications have been explored for increasing metal detection sensitivity. One common approach has been to incorporate graphene in the working electrode due to its unique thermal, mechanical, electrochemical properties [16]; moreover, graphene is thought to improve charge transfer processes. Graphene also has a large surface area compared to other carbon allotropes, and has been explored as a material for electrochemical nanocomposites [3,17,18]. For electrochemical applications, graphene-based polyaniline (G/PANI) nanocomposites have attracted more attention than pure graphene because the composite form is more compatible for electrode fabrication and functionalization [19,20]. Polyaniline (PANI) also has excellent electrochemical properties, is easily synthesized, functionalized, has good environmental stability, and is relatively nontoxic [21]. Consequently, PANI has been used for a variety of electronic, optical, and electrochemical applications [17,22]. Most G/PANI nanocomposites are prepared by in situ chemical oxidation polymerization and can contain covalent or noncovalent residues [23]. By controlling reaction conditions, G/PANI nanocomposites with different structures (e.g., nanospheres, nanorods, and nanowires) can be obtained [22]. Nanoparticle aggregation during synthesis has been prevented by adding polyvinylpyrrolidone (PVP) by a method called reverse dropping which creates a solution

of well-dispersed particles [24]. Here, the reverse dropping method with PVP was used, with modifications, to prepare G/PANI nanocomposites. Electrode modification has been accomplished in several ways, such as drop-casting [18], electrodeposition [10], and electrospinning/spraying [19,20]. In this work, electrospinning was selected as the modification method because it produces particles with a large specific surface area that can potentially provide ultra-high sensitivity and a fast electron transfer for electrochemical detection [19,20].

Two materials (plastic film and filter paper) were investigated as potential low-cost substrates for measuring Zn(II), Cd(II), and Pb(II) via anodic stripping voltammetry using G/PANI modified electrodes. Drop-casting and electrospinning were compared for electrode modification with the G/PANI nanocomposite. Signal interference from non-target metals was also investigated and found to have minimal impact on the resulting measurements. Finally, a demonstration of electrode selectivity for detection of all three heavy metals in complex media was performed using a human serum sample.

2. Experimental

2.1. Materials and methods

Standard solutions of all metals (Zn(II), Cd(II), Pb(II) Mn(II), and Bi(III)), cobalt(II) chloride, iron(III) chloride hexahydrate, copper(II) sulfate pentahydrate, and nickel(II) sulfate hexahydrate were purchased from Sigma–Aldrich (St. Louis, MO). Carbon ink (E3178, Ercon Incorporated, Wareham, MA) and graphite powder (diameter <20 μ m, Sigma–Aldrich, St. Louis, MO) were used for electrode fabrication. Graphene nanopowders were purchased from SkySpring Nanomaterials (Houston, TX), aniline monomer and PVP from Sigma–Aldrich (St. Louis, MO), trimethylsilylated Nafion[®] was from Aldrich Chem. Co. (Milwaukee, WI) and *N,N*-dimethylformamide (DMF) was from Carlo Erba Reagents (Milano, Italy). Transparency films (model number PP2200, 3M) and filter paper (Whatman grade 1) were purchased from Apollo Presentation Products (Booneville, MS) and GE Healthcare Bio-Sciences (Pittsburgh, PA), respectively. Sodium acetate and glacial acetic acid were obtained from Fisher Scientific (Pittsburgh, PA). Milli-Q water from Millipore ($R \geq 18.2$ M Ω cm⁻¹) was used for all experiments. All chemicals were used as received without further purification. Lyophilized human serum (CONSER, Nissui Pharmaceutical, Tokyo, Japan) was used to measure Zn(II), Cd(II), and Pb(II).

2.2. Preparation of the G/PANI nanocomposite

To prepare the G/PANI nanocomposite, 1.0 g aniline monomer was dissolved in 1.0 mL concentrated HCl and diluted to 10.0 mL total volume with DI H₂O (solution I). Graphene (10 mg) was next added to solution I and sonicated for 2 h to obtain a dispersed graphene–aniline monomer solution. In a separate beaker, 0.8 mL concentrated HCl, 1.0 g ammonium persulfate (APS), and 2.0 g PVP were dissolved in a total of 90.0 mL DI H₂O (solution II). Solution II was then cooled in an ice water bath for 30 min. Solutions I and II were mixed under vigorous stirring, continuously, for 4 h to obtain

a powder precipitate. The precipitate was filtered using 0.22 μm nylon membranes filter from Sigma–Aldrich (St. Louis, MO), rinsed with DI H_2O and EtOH until the filtrate became colorless, and then dried (on the filter) overnight at 65 °C. To confirm that G/PANI was completely doped with HCl, the dried powder was re-dispersed in 0.1 M HCl under ultrasonication for 30 min, filtered again, and dried [24]. Preparation of the G/PANI nanocomposite is shown in Scheme 1A. The G/PANI nanocomposite modified electrode was characterized using a JSM-6400 field emission scanning electron microscope (Japan Electron Optics Laboratory Co., Ltd., Japan) with an accelerating voltage of 15 kV and Fourier transform infrared spectroscopy (Nicolet 6700) from Nicolet, USA with a frequency of 400–4000 cm^{-1} using TGS detector (32 scans at resolution 4 cm^{-1}).

2.3. Fabrication of electrochemical sensors

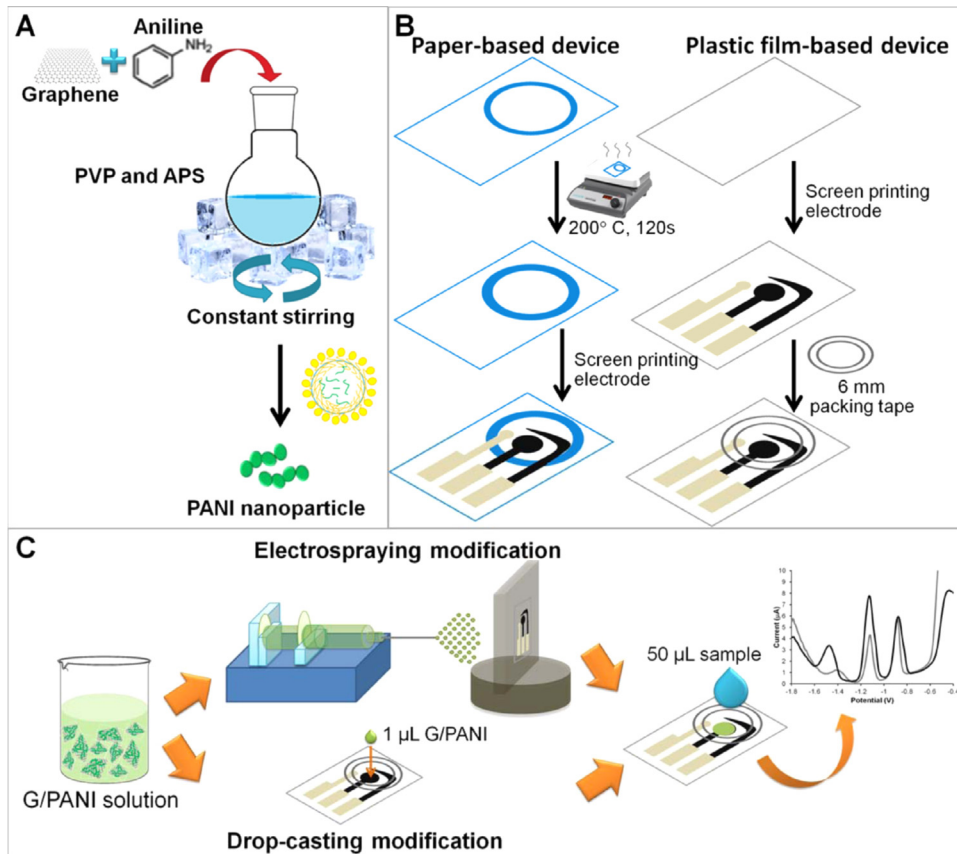
Electrodes were screen-printed according to previous methods, with slight modifications (Scheme 1B) [15]. Electrode designs were created with computer-aided design software (Adobe Illustrator). Hydrophobic barriers for confining aqueous media in filter paper were constructed by printing solid wax with a commercial printer (ColorQube 8870, Xerox, Japan) and melting the wax at 200 °C for 120 s on a hot plate. After hydrophobic barrier creation, electrodes (working, counter, and pseudo reference) and conductive pads were patterned on the substrate (film or paper) by screen-printing using carbon ink mixed with 5% (w/w) graphite powder. The screen-printed electrode was dried at 65 °C for 30 min to remove any remaining solvent [20]. On transparency film, a hydrophobic barrier for confining liquid was created by laser-cutting a ring out of common packing tape (6 mm inner diameter and 9 mm outer

diameter) and placing it in the middle of a screen-printed device to create a 3 mm diameter circle of exposed working electrode as shown in Scheme 1B. For the paper substrate, packing tape was placed on the back of the device after screen-printing (and heating) to prevent fluid leakage.

2.4. Electrode modification: drop-casting and electro spray methods

Before electrode modification, the G/PANI nanocomposite was dispersed in a PVP/DMF solution prepared by dissolving 2.0 mg mL^{-1} PVP in 98% DMF. The dispersed solution was probe-sonicated for 2 h at room temperature, after which 0.1% (v/v) polystyrene was added. For electrode modification via drop-casting, 1.0 μL of the dispersed G/PANI solution was dropped onto the working electrode and allowed to dry completely at room temperature (~ 10 min).

A custom-built electro spray system was used for electrode modification. The apparatus consisted of a syringe pump, high-voltage power supply, ground collector (5 cm from the needle tip), plastic syringe and stainless-steel needle. A 3.0 mL plastic syringe with a 26 G blunt needle was loaded with composite solution and inserted into a variable speed syringe pump (Kent Scientific Corp., Torrington, CT, U.S.A.) with a flow rate of 3.0 mL h^{-1} . Voltage control was performed using a high-voltage power supply (Gamma High Voltage Research, OrmondBeach, FL, U.S.A.). In this study, 14 kV of applied voltage, 5 min of spraying time, and 5 mg mL^{-1} of G/PANI in DMF were used for all experiments. A well-mixed G/PANI nanocomposite solution was sprayed onto the working electrode (WE) attached to a ground collector; the counter (CE) and reference electrodes (RE) were covered with aluminum foil to prevent spray from the process. To enhance detection



Scheme 1. Schematic drawing of (A) the preparation of the G/PANI nanocomposite, (B) electrochemical sensor fabrication on plastic film or paper, and (C) drop-casting and electro-spraying processes.

sensitivity of Zn(II), Cd(II), and Pb(II), 1.0 μL of Nafion was drop-cast on the G/PANI nanocomposite-modified electrode to pre-concentrate metal ions (Scheme 1C).

2.5. Electrochemical measurement

Electrochemical sensor performance was evaluated on both plastic and paper substrates by cyclic voltammetry (CV) and square-wave anodic stripping voltammetry (SWASV). A potentiostat (CHI 660B, CH Instruments, Austin, TX) controlled all electroanalytical measurements. For cyclic voltammetry, standard solutions of 2 mM ferri/ferricyanide were used; the potential was swept from -0.8V to $+0.7\text{V}$ with a scan rate of 100 mV s^{-1} . SWASV was used for the detection of Zn(II), Cd(II), and Pb(II) after dropping $50.0\text{ }\mu\text{L}$ of standard metals and $2.5\text{ }\mu\text{L}$ of 10.0 mg L^{-1} Bi(III) in 0.1 M acetate buffer pH 4.5 onto the three electrode system. In the pre-concentration step, Zn(II), Cd(II), and Pb(II) concentrations from 25.0 to $200.0\text{ }\mu\text{g L}^{-1}$ were accumulated on the electrode surface by applying a deposition potential of -1.6V for 240 s and 0.5 mg L^{-1} Bi(III) in situ. After 5 s of equilibration time, square-wave voltammograms with a frequency of 10 Hz, a step potential of 5 mV, and pulse amplitude of 25 mV were recorded from -1.8V to 0V .

2.6. Preparation of human serum samples

Prior to analysis, 3.0 mL of DI H_2O was added to lyophilized human serum. The serum was diluted ten-fold with 0.1 M sodium acetate buffer (pH 4.5). Heavy metals Zn(II), Cd(II), and Pb(II) were added by standard addition prior to experiments.

3. Results and discussion

3.1. Electrode characterization on paper and plastic substrates

The surface roughness of screen-printed carbon electrodes on paper and plastic surfaces was evaluated by optical profilometry. This method can resolve nanometer-sized features, which is helpful for identifying small differences in electrode surface structure. As shown in Fig. 1, on paper, the carbon electrode penetrated into the porous capillary network; consequently, the paper fibers and electrode surface are nearly indistinguishable. Conversely, the electrode is easily visualized when screen-printed on plastic because the carbon ink is retained on the substrate surface. The electrochemical performance of screen-printed carbon electrodes on paper and plastic surfaces, as evaluated by CV, is shown in Fig. S1. The peak potential difference of the electrode on plastic is lower for paper, indicating that electron transfer kinetics are faster for electrodes screen-printed on plastic. The SWASV responses of Zn(II), Cd(II), and Pb(II) on electrodes of identical composition were recorded with both substrates (Fig. 1C). Peak currents for electrodes on plastic are clearly improved over those on paper. Two possible explanations for the improvements are improved conductivity and higher surface roughness. On paper, the electrode material wicked into the substrate along porous fibers, generating thinner layers and higher electrode resistance. The degree of wicking would change based on fiber purity, ambient temperature, and also relative humidity, ultimately affecting the electrode from batch to batch. The electrode printed on plastic was also rougher, which could generate a higher current response than electrodes on paper for the detection of Zn(II), Cd(II), and Pb(II). As a result, we used a plastic substrate for all subsequent experiments to improve the electrochemical sensitivity of the system for Zn(II), Cd(II), and Pb(II) ions. Plastic substrates are marginally more expensive than paper, but provide better sensitivity, higher fabrication reproducibility, and are more resistant to mechanical

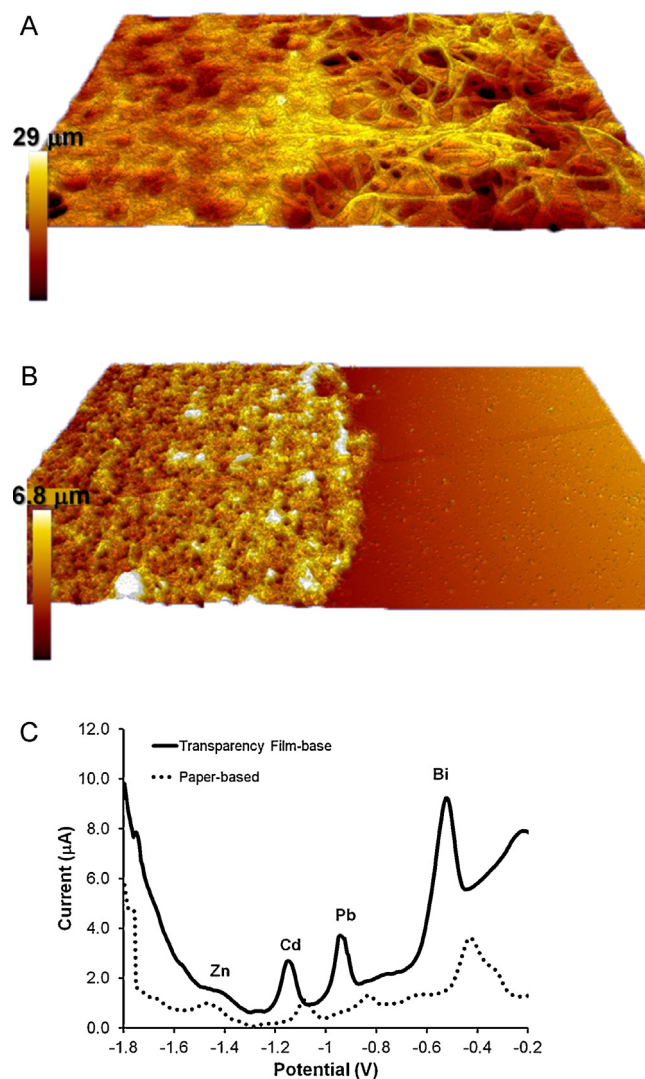


Fig. 1. Optical profile of a carbon working electrode on (A) filter paper and (B) a plastic transparency film. (C) SWASV of $200\text{ }\mu\text{g L}^{-1}$ Zn(II), Cd(II), and Pb(II) in 1.0 M acetate buffer pH 4.5 measured with a carbon electrode (3 mm diameter) on paper and plastic substrates.

fracture from bending and twisting than paper. Additionally, plastic does not degrade over time from contact with aqueous media.

3.2. G/PANI nanocomposite characterization

The granular morphology of synthesized PANI nanoparticles was characterized by SEM (Fig. 2A). A stabilizer, PVP, was used to increase the dispersion of PANI nanoparticles. To improve the conductivity and electroactivity of PANI nanoparticles, 10 mg of graphene was added to the aniline monomer solution. As seen in Fig. 2B, the G/PANI composite particles were slightly more monodisperse than PANI nanoparticles. The average diameter of PANI nanoparticles was $391 \pm 8\text{ nm}$ compared to $371 \pm 6\text{ nm}$ for G/PANI particles. A larger surface area-to-volume ratio of the nanocomposites increased signal-to-noise for SWASV relative to unmodified or PANI-modified electrodes. The particles were further characterized using Fourier transform infrared spectroscopy (Fig. 2C). The spectrum of G/PANI exhibited almost the same vibrational bands as pure PANI, however; the deviations from the characteristic band for G/PANI at 1240 , 1303 , and 3206 cm^{-1} can be attributed to molecular interaction between graphene and PANI

[25,26]. These results confirmed that PANI formed a composite particle with graphene.

3.3. Electrochemical characterization of the G/PANI composite-modified electrode

Graphene incorporation into PANI is crucial for improving the electrochemical properties of the nanocomposite. Drop-casting and electrospaying were investigated as methods for electrode surface functionalization. As shown in Fig. S2, the G/PANI nanocomposite-modified electrodes generated from both methods increased electrochemical sensitivity when measuring $200 \mu\text{g L}^{-1}$ of Zn(II), Cd(II), and Pb(II). Electrospaying displayed the best sensitivity, likely due to more uniform particle distribution as compared to drop-casting; moreover, electrospaying produced particles with greater surface-to-volume ratios [27,28].

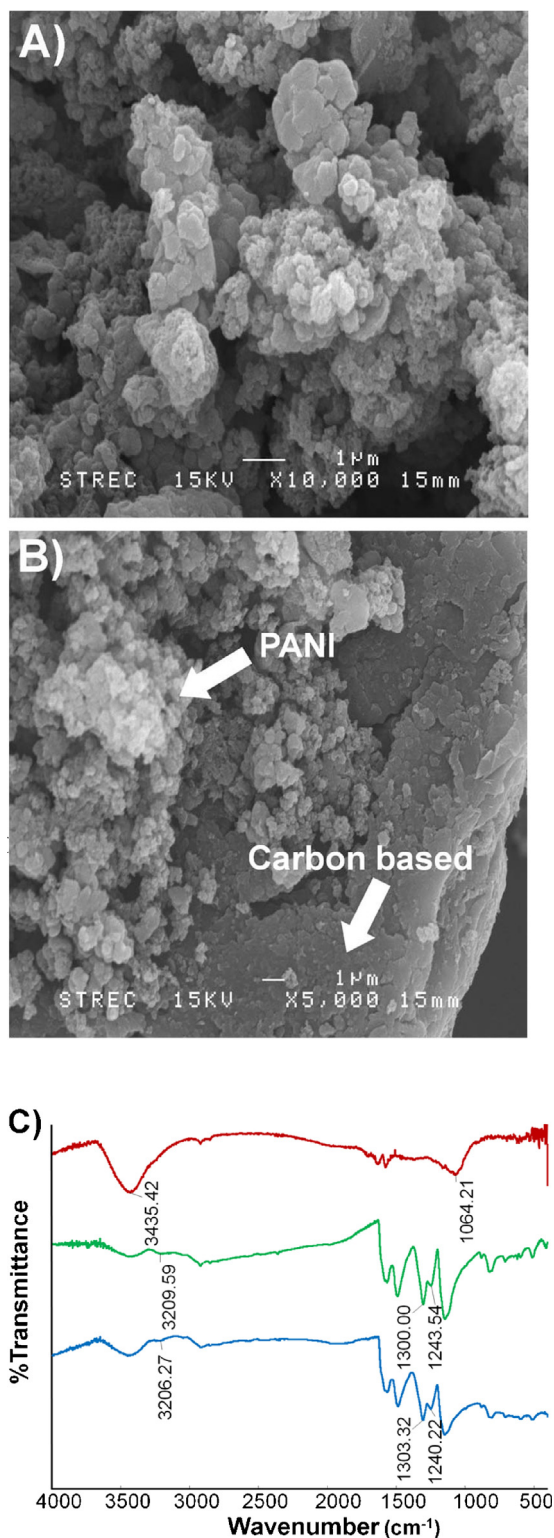


Fig. 2. Electrode surface characterization. (A) SEM micrographs of PANI nanoparticles and (B) G/PANI nanoparticles. (C) FT-IR spectrum of graphene (red line), PANI (green line), and the G/PANI nanocomposite (blue line). (For interpretation of the references to color in this figure legend, the reader is referred to the web version of this article.)

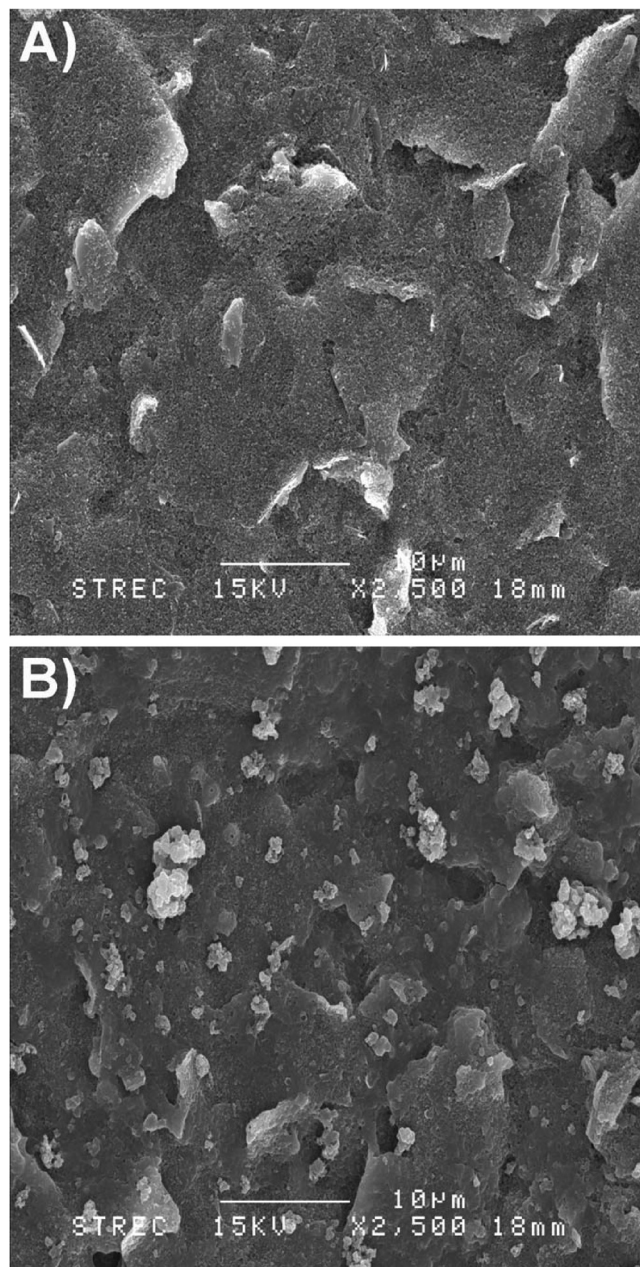


Fig. 3. SEM of an (A) unmodified and (B) G/PANI nanocomposite-modified electrode by electrospay.

The morphology of electrospayed and unmodified electrodes was also characterized by SEM (Fig. 3). The droplet-like structure of the G/PANI nanocomposite is relatively homogeneous over the electrode and has high surface coverage. The effect of graphene loading during synthesis was also investigated and optimized by cyclic voltammetry using $[\text{Fe}(\text{CN})_6]^{3-/4-}$ (Fig. S3). Anodic peak current increased when loaded with additional graphene from 0.0 to 10.0 mg, indicating that incorporating graphene into PANI significantly improved electrical conductivity. However, the anodic peak current subsequently decreased when graphene loading was higher than 10.0 mg. We suspect this decrease in oxidative current was from agglomeration of graphene at higher concentrations.

The performance of modified and unmodified electrodes (Fig. 4A) was investigated by cyclic voltammetry of $[\text{Fe}(\text{CN})_6]^{3-/4-}$ at scan rates between 25 and 300 mV s^{-1} . The largest anodic and cathodic currents were observed with the G/PANI nanocomposite-modified electrode, indicating that the cooperation of graphene and PANI improves the conduction pathway on the electrode surface. Moreover, the peak potential difference (ΔE_p) of the G/PANI ($\Delta E_p = 0.347 \text{ V}$) and PANI modified electrodes ($\Delta E_p = 0.377 \text{ V}$) decreased compared to ΔE_p of the unmodified electrode ($\Delta E_p = 0.517 \text{ V}$), further indicating that the presence of graphene and PANI improves electron transfer kinetics. The linearity of the anodic and cathodic peak currents versus the square root of scan rate verifies the redox process is controlled by diffusion (Fig. S4).

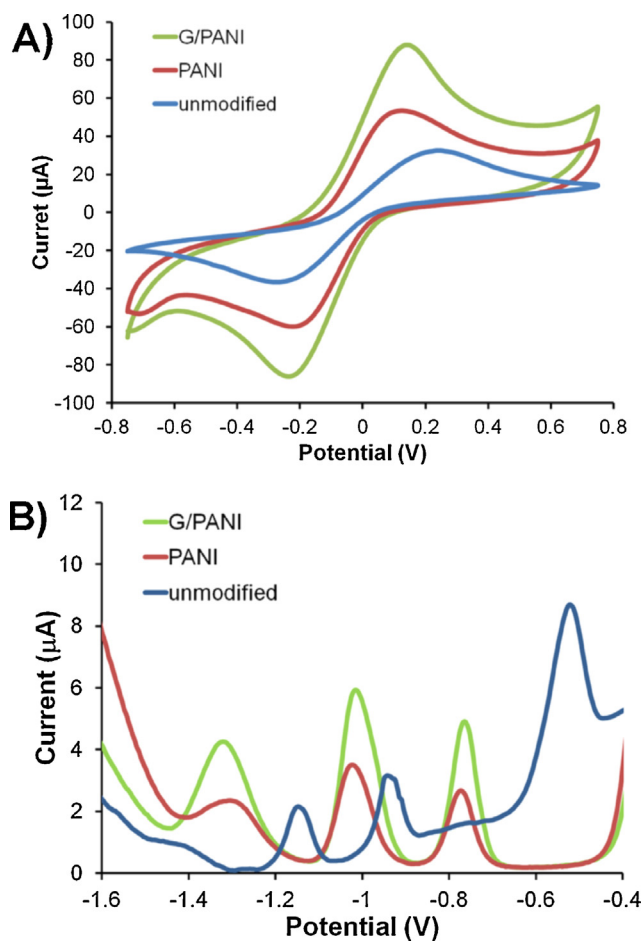


Fig. 4. (A) Cyclic voltammogram of 2.0 mM ferri/ferrocyanide in 0.1 M KCl and (B) square-wave voltammogram of $200 \mu\text{g L}^{-1}$ of Zn(II), Cd(II), and Pb(II) in 1.0 M acetate buffer pH 4.5 measured on an unmodified electrode, or electrodes functionalized with PANI or G/PANI nanocomposite solutions.

Next, SWASV was performed for Zn(II), Cd(II), and Pb(II) with electrodes that were unmodified or were functionalized with either G/PANI nanocomposites or PANI nanoparticles (Fig. 4B). The peak currents obtained for the three experiments demonstrated that the presence of the PANI nanoparticles increased electron transfer and that adding graphene further enhanced the signal (peak currents of Zn, Cd, and Pb increased 54%, 23%, and 42%, respectively).

3.4. Electrochemical detection of Zn(II), Cd(II), and Pb(II)

To detect very low levels of Zn(II), Cd(II), and Pb(II), SWASV is used because of its high sensitivity and linearity [3,29]. To increase electrode sensitivity, Bi was used to form a metal-Bi alloy on the electrode surface to facilitate the process of nucleation during metal ion deposition [9,30,31]. Moreover, the presence of a Nafion film on the electrode can further improve electrode sensitivity because negatively charged sulfonate groups in the Nafion film further preconcentrates metal cations [30,32,33]. Anodic peak potentials for Zn(II), Cd(II), and Pb(II) were measured at -1.31 ± 0.03 , -0.98 ± 0.04 , and $-0.75 \pm 0.04 \text{ V}$, respectively. Anodic peak currents of the three metals using electrodes modified with G/PANI and Nafion are showed in Fig. S5 (Supporting information). The resulting calibration

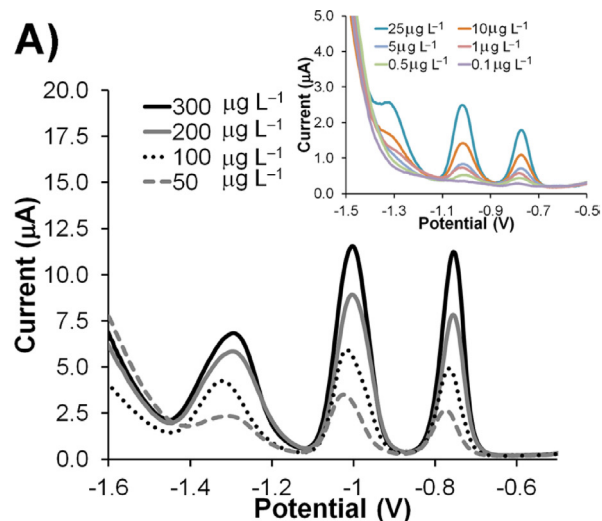


Figure 5B

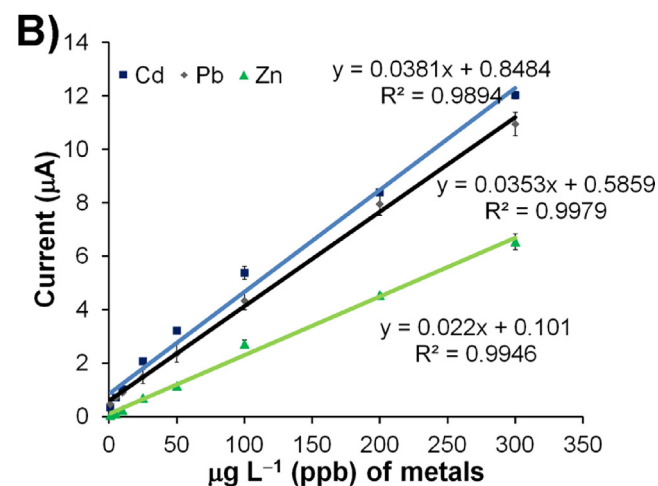


Fig. 5. (A) Square-wave voltammogram of Zn(II), Cd(II), and Pb(II) from 50–300 ppb. Results with metals of lower concentration (0.1–25 ppb) are shown in the inset. (B) Representative calibration graph for Zn(II), Cd(II), and Pb(II).

plots, (Fig. 5), are linear over a range from 1.0 to 300 $\mu\text{g L}^{-1}$ with correlation coefficients exceeding 0.98 for all metals. The experimentally determined limits of detection (LOD) for the system evaluated were 1.0 $\mu\text{g L}^{-1}$ for Zn(II) and 0.1 $\mu\text{g L}^{-1}$ for Cd(II) and Pb(II) based on signal-to-noise ratios for peak height of three ($S/N=3$). The analytical performance of all three metals is summarized in Table 1. G/PANI nanocomposite-modified electrodes coated with Nafion film provide sensitive, selective, and simultaneous analysis of all three metals.

Electrochemical performance of the G/PANI nanocomposite-modified electrode was compared with similar systems in the literature for measuring Zn(II), Cd(II), and Pb(II) (Table 1). Although the LOD presented in this work is comparable to other reports, the linear range obtained with our modification process is 1–2 orders of magnitude larger than most. Although the bimetallic Hg–Bi/SWNTs composite modified glassy carbon electrode [9] provides a lower LOD, Hg is toxic and its use has been discouraged. These comparisons suggest that our functionalization procedure could be promising when applied in more complex sample matrices such as human serum.

3.5. Interference study for Zn(II), Cd(II), and Pb(II) detection

The presence of non-target metals in solution can interfere with SWASV determination of heavy metals, so the tolerance ratio for common interfering metals (Mn(II), Cu(II), Fe(III), Fe(II), Co(III), and Ni(II)) was investigated [9,12]. The concentration of each species tested is provided in Table S1. A metal concentration altering an analyte peak current by >5% was considered inhibitory [12]. By limiting the scanning potential in the system from –1.6 to –0.5 V, we do not observe appreciable interference from metals at the concentrations listed in Table S1. Without additional electrode modification, the G/PANI nanocomposite-modified electrode was not affected by other metal species, demonstrating the selectivity of this electrode for Zn(II), Cd(II), and Pb(II).

3.6. Modified electrode reproducibility and stability

The reproducibility and stability of the Nafion-coated G/PANI nanocomposite-modified electrodes was next investigated by measuring the SWASV response of a 200 $\mu\text{g L}^{-1}$ solution composed of Zn(II), Cd(II), and Pb(II) in acetate buffer (pH 4.5). The RSD for anodic peak currents from 10 successive measurements using a single device was measured and found to be 9.2, 7.8, and 4.8% for Zn(II), Cd(II), and Pb(II), respectively. A similar experiment was performed with three devices and the RSD was 14.5, 12.9, and 7.25% for Zn(II), Cd(II), and Pb(II), respectively. To investigate electrode performance after periods of extended storage, devices were fabricated and kept in the dark at standard temperature and humidity for three weeks. After storage, the anodic current response retained $82 \pm 2\%$ of the initial response, with the decrease in performance likely from hydrolysis of the auxiliary electrode [10]. However, our sensor is ultimately intended to be low cost and disposable; therefore the loss of sensitivity after storage is not a performance limitation given our ability to detect very low levels of the target analytes even after signal loss.

3.7. Sample analysis

To demonstrate method applicability, Nafion-coated G/PANI nanocomposite electrodes were used for detecting Zn(II), Cd(II), and Pb(II) in human serum. In a healthy adult, blood levels of Zn, Cd, and Pb are typically at or below 900 $\mu\text{g L}^{-1}$ (18 μM), 29.7 $\mu\text{g L}^{-1}$, and 200 $\mu\text{g L}^{-1}$ (1 μM), respectively [34]. For our analysis, human serum was diluted (1:10) with acetate buffer (pH 4.5) and spiked with three different concentrations of Zn (II), Cd(II), and Pb(II). Each sample was analyzed in triplicate and the results summarized in Table 2. Recoveries ranged from 93.8 to 109.7% and the RSD ($n=3$) was below 9.0%, indicating that the system is accurate and reproducible.

Table 1
Electrode performance for measuring Zn(II), Cd(II), and Pb(II).

Modified electrode	Detection limit ($\mu\text{g L}^{-1}$)			Linear range ($\mu\text{g L}^{-1}$)			Ref.
	Zn	Cd	Pb	Zn	Cd	Pb	
Bimetallic Hg–Bi/SWNTs composite/GCE	0.23	0.076	0.18	0.5–11	0.5–11	0.5–11	[9]
SnO ₂ /reduced graphene oxide nanocomposite	–	0.0001015	0.0001839	–	0.0003–0.0012	0.0003–0.0012	[18]
CNTs	–	5–150	5–150	–	1	1	[12]
CNT arrays (CNT thread)	1.4	1.8	1.5	3–9	1.5–4.5	1–4	[35]
Bismuth/poly(<i>p</i> -aminobenzene sulfonic acid)	0.62	0.63	0.8	1–110	1–110	1–130	[36]
Nitrogen-doped microporous carbon/Nafion/bismuth-film electrode	–	1.5	0.05	–	2–10, 10–100	0.5–10, 10–100	[37]
Bi/Au–GN–Cys/GCE	–	0.1	0.05	–	0.50–40	0.50–40	[38]
Bi/Nafion/PANI–MES/GCE	–	0.04	0.05	–	0.10–20	0.10–30	[39]
Clioquinol/HMDE	0.06	0.06	0.1	0–25	0–15	0–15	[40]
Screen-printed carbon nanotubes electrodes	11	0.8	0.2	12–100	2–100	2–100	[7]
Nafion/G/PANI nanocomposite	1.0	0.1	0.1	1–300	1–300	1–300	This work

Table 2
Determination of Zn(II), Cd(II), and Pb(II) in human serum samples ($n=3$).

Added concentration ($\mu\text{g L}^{-1}$)	Measured concentration ($\mu\text{g L}^{-1}$)			% recovery	% RSD
	Zn(II)	Cd(II)	Pb(II)		
10.0	9.41 \pm 0.5	10.7 \pm 0.5	10.6 \pm 0.4	94.1 – 106.5	4.0 – 4.8
20.0	19.5 \pm 1.7	20.2 \pm 1.7	18.8 \pm 1.1	93.8 – 101.1	3.4 – 8.5
50.0	51.1 \pm 2.2	54.9 \pm 4.8	52.7 \pm 3.0	102.3 – 109.	4.3 – 8.8

4. Conclusions

Transparency film and paper-based electrodes modified with G/PANI were compared for the determination of Zn(II), Cd(II), and Pb(II). The high conductivity and large surface area of the droplet-like structures of the G/PANI nanocomposites deposited by electrospray on polymer electrodes significantly improved electrochemical sensitivity. Additionally, using Nafion on the G/PANI nanocomposite-modified electrode increased sensitivity for measuring Zn(II), Cd(II), and Pb(II). Under optimal conditions, detection limits at or below 1 ppb and wide linear ranges (>2 orders of magnitude) were obtained for Zn(II), Cd(II), and Pb(II). Nafion-coated electrodes modified with the G/PANI nanocomposite solution were then used to measure the metals in human serum and showed good collection efficiency. These results demonstrate the electrode as a low-cost alternative solution for determination of heavy metals.

Acknowledgments

The authors gratefully acknowledge financial support from the Chulalongkorn University Dutsadi Phiphat Scholarship and the Thailand Research Fund (TRF) through the New Researchers Grant. We also thank the Ratchadaphiseksomphot Endowment Fund 2013 of Chulalongkorn University (CU-56-640-HR). Additional support was provided by the National Institute for Occupational Safety and Health (OH010050). Finally, we would also like to thank Dr. Melissa Reynolds, Department of Chemistry and School of Biomedical Engineering, Colorado State University, CO, USA, for use of the electrospraying equipment.

Appendix A. Supplementary data

Supplementary data associated with this article can be found, in the online version, at <http://dx.doi.org/10.1016/j.aca.2015.02.064>.

References

- [1] S.S. Lim, T. Vos, A.D. Flaxman, G. Danaei, K. Shibuya, H. Adair-Rohani, M.A. AlMazroa, M. Amann, H.R. Anderson, K.G. Andrews, M. Aryee, C. Atkinson, L.J. Bacchus, A.N. Bahalim, K. Balakrishnan, J. Balmes, S. Barker-Collo, A. Baxter, M. L. Bell, J.D. Blore, F. Blyth, C. Bonner, G. Borges, R. Bourne, M. Boussinesq, M. Brauer, P. Brooks, N.G. Bruce, B. Brunekreef, C. Bryan-Hancock, C. Bucello, R. Buchbinder, F. Bull, R.T. Burnett, T.E. Byers, B. Calabria, J. Carapetis, E. Carnahan, Z. Chafe, F. Charlson, H. Chen, J.S. Chen, A.T.-A. Cheng, J.C. Child, A. Cohen, K.E. Colson, B.C. Cowie, S. Darby, S. Darling, A. Davis, L. Degenhardt, F. Dentener, D. C. Des Jarlais, K. Devries, M. Dherani, E.L. Ding, E.R. Dorsey, T. Driscoll, K. Edmond, S.E. Ali, R.E. Engell, P.J. Erwin, S. Fahimi, G. Falder, F. Farzadfar, A. Ferrari, M.M. Finucane, S. Flaxman, F.G.R. Fowkes, G. Freedman, M.K. Freeman, E. Gakidou, S. Ghosh, E. Giovannucci, G. Gmel, K. Graham, R. Grainger, B. Grant, D. Gunnell, H.R. Gutierrez, W. Hall, H.W. Hoek, A. Hogan, H.D. Hosgood III, D. Hoy, H. Hu, B.J. Hubbell, S.J. Hutchings, S.E. Ibeanusi, G.L. Jacklyn, R. Jasrasaria, J. B. Jonas, H. Kan, J.A. Kanis, N. Kassebaum, N. Kawakami, Y.-H. Khang, S. Khatibzadeh, J.-P. Khoo, C. Kok, F. Laden, R. Lalloo, Q. Lan, T. Lathlean, J.L. Leasher, J. Leigh, Y. Li, J.K. Lin, S.E. Lipshultz, S. London, R. Lozano, Y. Lu, J. Mak, R. Malekzadeh, L. Mallinger, W. Marcenes, L. March, R. Marks, R. Martin, P. McGale, J. McGrath, S. Mehta, Z.A. Memish, G.A. Mensah, T.R. Merriman, R. Micha, C. Michaud, V. Mishra, K.M. Hanafiah, A.A. Mokdad, L. Morawska, D. Mozaffarian, T. Murphy, M. Naghavi, B. Neal, P.K. Nelson, J.M. Nolla, R. Norman, C. Olives, S.B. Omer, J. Orchard, R. Osborne, B. Ostro, A. Page, K.D. Pandey, C.D.H. Parry, E. Passmore, J. Patra, N. Pearce, P.M. Pelizzari, M. Petzold, M.R. Phillips, D. Pope, C.A. Pope III, J. Powles, M. Rao, H. Razavi, E.A. Rehfuess, J.T. Rehm, B. Ritz, F.P. Rivara, T. Roberts, C. Robinson, J.A. Rodriguez-Portales, I. Romieu, R. Room, L.C. Rosenfeld, A. Roy, L. Rushton, J.A. Salomon, U. Sampson, L. Sanchez-Riera, E. Sanman, A. Sapkota, S. Seedat, P. Shi, K. Shield, R. Shivakoti, G.M. Singh, D.A. Sleet, E. Smith, K.R. Smith, N.J.C. Stapelberg, K. Steenland, H. Stöckl, L.J. Stovner, K. Straif, L. Straney, G.D. Thurston, J.H. Tran, R. Van Dingenen, A. van Donkelaar, J.L. Veerman, L. Vijayakumar, R. Weintraub, M.M. Weissman, R.A. White, H. Whiteford, S.T. Wiersma, J.D. Wilkinson, H.C. Williams, W. Williams, N. Wilson, A.D. Woolf, P. Yip, J.M. Zielinski, A.D. Lopez, C.J.L. Murray, M. Ezzati, A comparative risk assessment of burden of disease and injury attributable to 67 risk factors and risk factor clusters in 21 regions, 1990–2010: a systematic analysis for the Global Burden of Disease Study 2010, *Lancet* 380 (2012) 2224–2260.
- [2] D. Loomis, Y. Grosse, B. Lauby-Secretan, F.E. Ghissassi, V. Bouvard, L. Benbrahim-Tallaa, N. Guha, R. Baan, H. Mattock, K. Straif, The carcinogenicity of outdoor air pollution, *Lancet Oncol.* 14 (2013) 1262–1263.
- [3] G. Aragay, A. Merkoçi, Nanomaterials application in electrochemical detection of heavy metals, *Electrochim. Acta* 84 (2012) 49–61.
- [4] M. Soyak, N. Kizil, Determination of some heavy metals by flame atomic absorption spectrometry before coprecipitation with neodymium hydroxide, *J. AOAC Int.* 94 (2011) 978–984.
- [5] J.V. Maciel, C.L. Knorr, E.M.M. Flores, E.I. Müller, M.F. Mesko, E.G. Primel, F.A. Duarte, Feasibility of microwave-induced combustion for trace element determination in *Engraulis anchoita* by ICP-MS, *Food Chem.* 145 (2014) 927–931.
- [6] E. Furia, D. Aiello, L. Di Donna, F. Mazzotti, A. Tagarelli, H. Thangavel, A. Napoli, G. Sindona, Mass spectrometry and potentiometry studies of Pb(II)-, Cd(II)- and Zn(II)-cystine complexes, *Dalton Trans.* 43 (2014) 1055–1062.
- [7] U. Injang, P. Noyrod, W. Siangproh, W. Dungchai, S. Motomizu, O. Chailapakul, Determination of trace heavy metals in herbs by sequential injection analysis-anodic stripping voltammetry using screen-printed carbon nanotubes electrodes, *Anal. Chim. Acta* 668 (2010) 54–60.
- [8] G.-J. Lee, C.K. Kim, M.K. Lee, C.K. Rhee, Simultaneous voltammetric determination of Zn, Cd and Pb at bismuth nanopowder electrodes with various particle size distributions, *Electroanalysis* 22 (2010) 530–535.
- [9] R. Ouyang, Z. Zhu, C.E. Tatum, J.Q. Chambers, Z.-L. Xue, Simultaneous stripping detection of Zn(II), Cd(II) and Pb(II) using a bimetallic Hg-Bi/single-walled carbon nanotubes composite electrode, *J. Electroanal. Chem.* 656 (2011) 78–84.
- [10] P. Jothimuthu, R. Wilson, J. Herren, E. Haynes, W. Heineman, I. Papautsky, Lab-on-a-chip sensor for detection of highly electronegative heavy metals by anodic stripping voltammetry, *Biomed. Microdevices* 13 (2011) 695–703.
- [11] A. Krolicka, A. Bobrowski, K. Kalcher, J. Mocak, I. Svancara, K. Vytras, Study on catalytic adsorptive stripping voltammetry of trace cobalt at bismuth film electrodes, *Electroanalysis* 15 (2003) 1859–1863.
- [12] P. Rattanarat, W. Dungchai, D. Cate, J. Volckens, O. Chailapakul, C.S. Henry, Multilayer paper-based device for colorimetric and electrochemical quantification of metals, *Anal. Chem.* 86 (2014) 3555–3562.
- [13] A. Apilux, W. Dungchai, W. Siangproh, N. Praphairaksit, C.S. Henry, O. Chailapakul, Lab-on-paper with dual electrochemical/colorimetric detection for simultaneous determination of gold and iron, *Anal. Chem.* 82 (2010) 1727–1732.
- [14] W. Dungchai, O. Chailapakul, C.S. Henry, Electrochemical detection for paper-based microfluidics, *Anal. Chem.* 81 (2009) 5821–5826.
- [15] M.M. Mentele, J. Cunningham, K. Koehler, J. Volckens, C.S. Henry, Microfluidic paper-based analytical device for particulate metals, *Anal. Chem.* 84 (2012) 4474–4480.
- [16] A.K. Geim, K.S. Novoselov, The rise of graphene, *Nat. Mater.* 6 (2007) 183–191.
- [17] C. Harish, V.S. Sreeharsha, C. Santhosh, R. Ramachandran, M. Saranya, T.M. Vanchinathan, K. Govardhan, A.N. Grace, Synthesis of polyaniline/graphene nanocomposites and its optical, electrical and electrochemical properties, *Adv. Sci. Eng. Med.* 5 (2013) 140–148.
- [18] Y. Wei, C. Gao, F.-L. Meng, H.-H. Li, L. Wang, J.-H. Liu, X.-J. Huang, SnO₂/reduced graphene oxide nanocomposite for the simultaneous electrochemical detection of cadmium(II), lead(II), copper(II), and mercury(II): an interesting favorable mutual interference, *J. Phys. Chem. C* 116 (2011) 1034–1041.
- [19] N. Rodthongkum, N. Ruecha, R. Rangkupan, R.W. Vachet, O. Chailapakul, Graphene-loaded nanofiber-modified electrodes for the ultrasensitive determination of dopamine, *Anal. Chim. Acta* 804 (2013) 84–91.
- [20] N. Ruecha, R. Rangkupan, N. Rodthongkum, O. Chailapakul, Novel paper-based cholesterol biosensor using graphene/polyvinylpyrrolidone/polyaniline nanocomposite, *Biosens. Bioelectron.* 52 (2014) 13–19.
- [21] C. Dhand, M. Das, M. Datta, B.D. Malhotra, Recent advances in polyaniline based biosensors, *Biosens. Bioelectron.* 26 (2011) 2811–2821.
- [22] L. Wang, X. Lu, S. Lei, Y. Song, Graphene-based polyaniline nanocomposites: preparation, properties and applications, *J. Mater. Chem. A* 2 (2014) 4491–4509.
- [23] D. Saini, T. Basu, Synthesis and characterization of nanocomposites based on polyaniline-gold/graphene nanosheets, *Appl. Nanosci.* 2 (2012) 467–479.
- [24] P. Zhang, X. Han, L. Kang, R. Qiang, W. Liu, Y. Du, Synthesis and characterization of polyaniline nanoparticles with enhanced microwave absorption, *RSC Adv.* 3 (2013) 12694–12701.
- [25] M. Parmar, C. Balamurugan, D.-W. Lee, PANI and graphene/PANI nanocomposite films-comparative toluene gas sensing behavior, *Sensors* 13 (2013) 16611–16624.
- [26] U. Rana, S. Malik, Graphene oxide/polyaniline nanostructures: transformation of 2D sheet to 1D nanotube and in situ reduction, *Chem. Commun.* 48 (2012) 10862–10864.
- [27] B. Ding, M. Wang, X. Wang, J. Yu, G. Sun, Electrospun nanomaterials for ultrasensitive sensors, *Futur. Today* 13 (2010) 16–27.
- [28] S. Ramakrishna, K. Fujihara, W.-E. Teo, T. Yong, Z. Ma, R. Ramaseshan, Electrospun nanofibers: solving global issues, *Mater. Today* 9 (2006) 40–50.
- [29] P.A. Dimovasilis, M.I. Prodromidis, Bismuth-dispersed xerogel-based composite films for trace Pb(II) and Cd(II) voltammetric determination, *Anal. Chim. Acta* 769 (2013) 49–55.

- [30] M. Li, D.-W. Li, Y.-T. Li, D.-K. Xu, Y.-T. Long, Highly selective in situ metal ion determination by hybrid electrochemical adsorption–desorption and colorimetric methods, *Anal. Chim. Acta* 701 (2011) 157–163.
- [31] M.Á.G. Rico, M. Olivares-Marín, E.P. Gil, Modification of carbon screen-printed electrodes by adsorption of chemically synthesized Bi nanoparticles for the voltammetric stripping detection of Zn(II), Cd(II) and Pb(II), *Talanta* 80 (2009) 631–635.
- [32] K. Keawkim, S. Chuanuwatanakul, O. Chailapakul, S. Motomizu, Determination of lead and cadmium in rice samples by sequential injection/anodic stripping voltammetry using a bismuth film/crown ether/Nafion modified screen-printed carbon electrode, *Food Control* 31 (2013) 14–21.
- [33] S. Legeai, O. Vittori, A Cu/Nafion/Bi electrode for on-site monitoring of trace heavy metals in natural waters using anodic stripping voltammetry: an alternative to mercury-based electrodes, *Anal. Chim. Acta* 560 (2006) 184–190.
- [34] L. Goullé, J. Mahieu, N. Castermant, L. Neveu, G. Bonneau, D. Lainé, C. Bouige, Metal and metalloid multi-elementary ICP-MS validation in whole blood, plasma, urine and hair, *Forensic Sci. Int.* 153 (2015) 39–44.
- [35] D. Zhao, X. Guo, T. Wang, N. Alvarez, V.N. Shanov, W.R. Heineman, Simultaneous detection of heavy metals by anodic stripping voltammetry using carbon nanotube thread, *Electroanalysis* 26 (2014) 488–496.
- [36] Y. Wu, N.B. Li, H.Q. Luo, Simultaneous measurement of Pb, Cd and Zn using differential pulse anodic stripping voltammetry at a bismuth/poly(*p*-aminobenzene sulfonic acid) film electrode, *Sens. Actuators B* 133 (2008) 677–681.
- [37] L. Xiao, H. Xu, S. Zhou, T. Song, H. Wang, S. Li, W. Gan, Q. Yuan, Simultaneous detection of Cd(II) and Pb(II) by differential pulse anodic stripping voltammetry at a nitrogen-doped microporous carbon/Nafion/bismuth-film electrode, *Electrochim. Acta* 143 (2014) 143–151.
- [38] L. Zhu, L. Xu, B. Huang, N. Jia, L. Tan, S. Yao, Simultaneous determination of Cd(II) and Pb(II) using square wave anodic stripping voltammetry at a gold nanoparticle–graphene–cysteine composite modified bismuth film electrode, *Electrochim. Acta* 115 (2014) 471–477.
- [39] L. Chen, Z. Su, X. He, Y. Liu, C. Qin, Y. Zhou, Z. Li, L. Wang, Q. Xie, S. Yao, Square wave anodic stripping voltammetric determination of Cd and Pb ions at a Bi/Nafion/thiolated polyaniline/glassy carbon electrode, *Electrochem. Commun.* 15 (2012) 34–37.
- [40] E. Herrero, V. Arancibia, C. Rojas-Romo, Simultaneous determination of Pb²⁺, Cd²⁺ and Zn²⁺ by adsorptive stripping voltammetry using clioquinol as a chelating-adsorbent agent, *J. Electroanal. Chem.* 729 (2014) 9–14.